Tikrit Journal of Pure Science Vol. 31 (3) 2026

DOI: *HTTPS://DOI.ORG/10.25130/TJPS.V31I3.1949*

IRAQI Academic Scientific Journals

Tikrit Journal of Pure Science

ISSN: 1813 – 1662 (Print) --- E-ISSN: 2415 – 1726 (Online)

Journal Homepage: https://tjpsj.org/

Tikrit Journal of Pure Science

Preparation of Copper Oxide Nanoparticles Using Pulsed Laser Ablation Method in Liquid at Different Energies and Study of Their Structural and Optical Properties

Omayma Saad Khalid, Awatif Sabir Jasim

Department of Physics, College of Science, University of Tikrit, Tikrit, Iraq

Received: 17 Mar. 2025 **Received in revised forum:** 20 May. 2025 **Accepted:** 25 May. 2025

Final Proofreading: 21 Jun. 2025 **Available online:** 25 Jun. 2026

ABSTRACT

In this study, copper oxide nanoparticles (CuO NPs) were prepared and characterized with the pulsed laser ablation in liquid (PLAL) technique using a wavelength (532 nm) of Nd: YAG laser, with different energies (100, 150, and 200 mJ) for ablation of the mineral copper target. Colloidal NPs have been characterized using the field-emission scanning electron microscope (FESEM), UV-Vis technique, and X-ray diffraction (XRD). The resulting colloidal CuO NP solutions were green. FESEM images showed that most of the NPs obtained across all laser energies have individualized needle shapes with sizes below 100 nm. Furthermore, samples prepared in deionized water showed average diameters of 22.153, 25.79, and 20.664 nm for CuO NPs. Results of XRD showed that CuO NPs showed a mono-inclined crystal structure. The visible UV spectrometry confirmed that the absorption values of CuO NPs increased as the laser effect increased, with the energy gap decreasing by (2.6 – 2.53 eV).

***Keywords*:** Ablation, CuO NPs, Energy gap, PLAL.

Name: Omayma Saad Khalid **E-mail:** omayma.s.khaled.phys608@st.tu.edu.iq

Tikrit Journal of Pure Science Vol. 31 (3) 2026
DOI: HTTPS://DOI.ORG/10.25130/TJPS.V31I3.1949

تحضير جسيمات اوكسيد النحاس النانوية باستخدام طريقة الاستئصال بالليزر النبضي في السائل بطاقات مختلفة ودراسة خصائصها التركيبية والبصرية

اميمه سعد خالد، عواطف صابر جاسم

قسم الفيزياء، كلية العلوم، جامعة تكريت، تكريت، العراق

الملخص

في هذه الدراسة، تم تحضير وتوصيف جسيمات أوكسيد النحاس النانوية (CuO NPs) بتقنية الاستئصال بالليزر النبضي في السائل (PLAL) باستخدام ليزر Nd: YAG بطول موجي (532 nm) بطاقات مختلفة (100, 150, 200 mJ) لاستئصال هدف معدن النحاس مغمور في ماء منزوع الايونات. تم توصيف الجسيمات النانوية الغروية باستخدام المجهر الإلكتروني الماسح الباعث للمجال (FESEM) وتقنية تحليل مطياف الأشعة فوق البنفسجية والمرئية (UV-Vis)، وحيود الأشعة السينية (XRD). تبين ان محاليل CuO NPs الغروانية الناتجة خضراء اللون. أظهرت صور المجهر FESEM أن معظم الجسيمات النانوية التي تم الحصول عليها من جميع طاقات الليزر المستخدمة لها اشكال منفردة ابرية بشكل تجمعات وتكتلات بحجم أقل من (100 nm). علاوة على ذلك، اظهرت نتائج العينات المحضرة في وسط الماء منزوع الايونات أن متوسط أقطار جسيمات اوكسيد النحاس النانوية (22.153, 25.79, and 20.664 nm). أظهرت نتائج حيود الأشعة السينية ان جسيمات أوكسيد النحاس النانوية ذات بنية بلورية احادية الميل. وأكدت أطياف الأشعة فوق البنفسجية –المرئية أن قيم الامتصاص لجسيمات أوكسيد النحاس النانوية زادت مع زيادة تأثير الليزر مع انخفاض فجوة الطاقة بمقدار (2.53 eV – 2.6).

INTRODUCTION

Nanotechnology has become a subject of modern science and is now the most important in physics, chemistry, life sciences and other fields. Nanomaterials are defined as distinct and unique materials that can be produced in scales ranging in size from 1-100 nm) [1] In recent developments, nanoparticles have been manufactured for various applications and fields and combined with other nanomaterials, thereby achieving high efficiency. [2]. Nanoparticles can be manufactured in three ways: physically, chemically or biologically. Chemical methods have adverse effects due to the presence of certain toxic chemicals absorbed on the surface. Environmentally friendly alternatives to chemical methods include physical methods, such as laser nanoparticle ablation.[2, 3]The pulsed laser ablation method in liquid is an easy, affordable and effective way to create a wide range of highly desirable materials. [4]. Nanoparticles of copper oxide (CuO NPs) are of great importance because of their optical, mechanical, electrical and medical properties used in wound bandages, highlighting recent developments in bioprocessory manufacturing of inorganic particles, including metal particles, oxide molecules and other particles to develop antimicrobials that can be useful in hospitals to prevent or reduce disease-causing bacteria. [5]. Nanoparticles have light sensitivity and electrical conductivity, making them applicable in various technological fields. [6]. Nanoparticles can be manufactured using various physical and chemical techniques, including laser removal. [7]. This work aims to evaluate the effect of energy on the synthetic and optical properties of nanoparticles prepared from a pure copper target using pulsed laser ablation in liquid.

MATERIALS AND METHODS

In this work, the PLAL technique using a Q-switched Nd: YAG laser was used to produce copper NPs. Metal plate surfaces (copper) were cleaned using deionized water before the ablation process began to eliminate impurities. Thereafter,

the metal plate with high purity dimensions (1 cm, 1 cm, and 2 mm) was inserted into the capacity (100 ml) along with (5 ml) of deionized water, as shown in Figure 1. The distance between the laser source and the sample was adjusted to 15 cm. The level of liquid above the sample (5 mm) was measured. The laser beam was directed vertically towards targets at different energies (100, 150, and 200 mJ) while maintaining a constant number of pulses (1000), a constant frequency (5 Hz), and a wavelength of 532 nm at room temperature. Structural and optical results were analyzed using OriginPro 2025 and ImageJ to determine NP size.

Fig. 1: Nd: YAG laser device.

RESULTS AND DISCUSSION

XRD Analysis

XRD pattern analysis was performed on copper oxide nanoparticles prepared in deionized water using PLAL. The results showed that the crystalline system of these NPs is mono-inclined. The most important structural parameters were found using the Scherer equation to calculate the crystalline size (D)[8]:

$$D = K\lambda/\beta\cos\theta \quad \ldots (1)$$

Where K is the constant of the relationship, λ is the wavelength (1.5406 Å), β is the full width at half maximum (FWHM), and θ is the Bragg angle. The distance between crystal levels (d_{hkl}) was calculated using the Bragg equation. [9]:

$$n\lambda = 2d_{hkl}\sin\theta \quad \ldots (2)$$

Where n is an integer representing the diffraction order, in Figure (2-a), eight peaks appeared at the angles (35.49º, 38.83º, 48.59º, 53.52º, 58.39º, 61.75º, 66.36º, and 75.39º) at the energy (100 mJ) consistent with the crystal levels (002), (200), (-202), (020), (202), (-113), (-311), and (-222), respectively. In Figure (2-b), eleven peaks were observed at the angles (32.39º, 35.49º, 38.92º, 46.32º, 48.66º, 53.45º, 58.29º, 61.54º, 66.24º, 68.12º and 74.96º) at the energy (150 mJ) correspond to the crystal levels (110), (002), (200), (-112), (-202), (020), (202), (-113), (-311), (220), and (004), respectively. In Figure (2-c) ten peaks were observed at angles (31.74º, 34.61º, 38.59º, 41.41º, 45.91º, 48.84º, 52.34º, 58.06º, 61.36º and 74.58º) at the energy (200 mJ) corresponding to the crystal levels (110), (002), (111), (-112), (-202), (020), (202), (-113), and (004), respectively. Increasing the laser energy reduces NP size and increases crystal stress, thereby shifting the diffraction peaks. XRD data are shown in Table 1. All of these results are highly consistent with the values listed on the ICDD card for copper oxide (00-005-0661). In addition, the crystalline content trend (002) is prevalent at all energies (100, 150, and 200 mJ). These results are also consistent with the results of a previous study, such as [10].

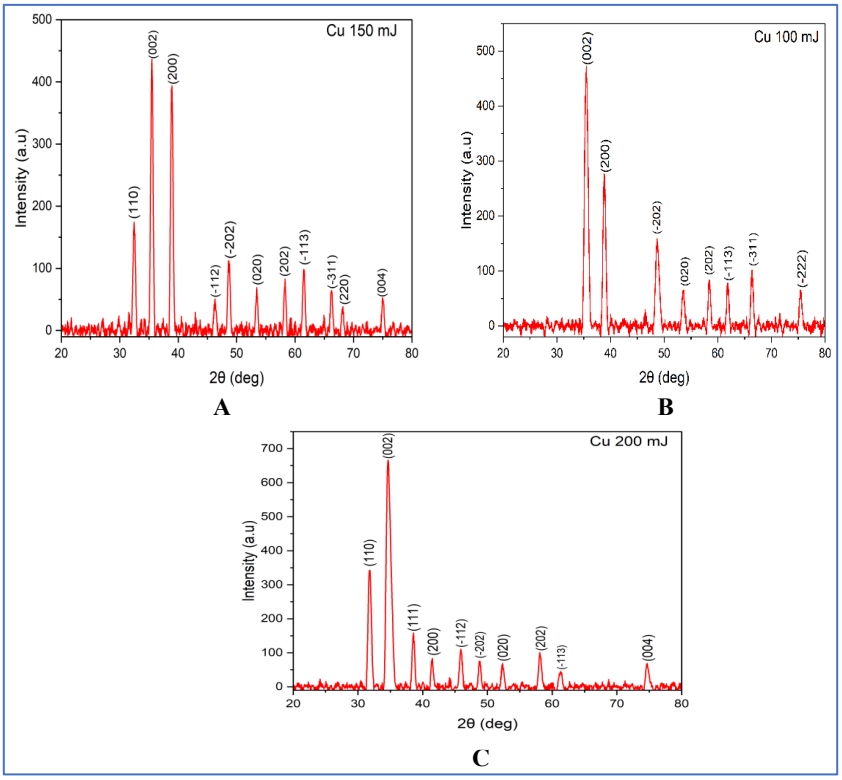

Fig. 2: XRD patterns of CuO NPs produced at energies: (a) 100 mJ, (b) 150 mJ, (c) 200 mJ.

Table 1: Experimental XRD results of the prepared CuO NPs.

Energy (mJ)	2θ (deg)	FWHM (deg)	d_{hkl} (Å)	D (nm)	hkl
100	35.4937	0.6888	2.52922	12.1	(002)
	38.8317	0.5904	2.31915	14.3	(200)
	48.5973	0.5412	1.87351	16.1	(-202)
	53.5225	0.492	1.71215	18.1	(020)
	58.39	0.3936	1.58049	23.1	(202)
	61.7566	0.3936	1.50217	23.5	(-113)
	66.3653	0.3936	1.40859	24.1	(-311)
	75.3967	0.492	1.26072	20.4	(-222)
150	32.3983	0.3936	2.76345	21.0	(110)
	35.4959	0.4428	2.52907	18.8	(002)
	38.9231	0.4428	2.31392	19.0	(200)
	46.3212	0.5904	1.96013	14.6	(-112)
	48.6695	0.3936	1.8709	22.2	(-202)
	53.4502	0.3936	1.7143	22.6	(020)
	58.2918	0.3444	1.58292	26.4	(202)
	61.5412	0.4428	1.50691	20.9	(-113)
	66.2471	0.3444	1.41082	27.5	(-311)
	68.1257	0.2952	1.37642	32.5	(220)
	74.9628	0.3936	1.26694	25.4	(004)
200	31.7426	0.5412	2.81901	15.3	(110)
	34.6114	0.6396	2.59165	13.0	(002)
	38.5948	0.4428	2.33284	19.0	(111)
	41.4139	0.3444	2.18033	24.7	(200)
	45.9148	0.3936	1.97653	21.9	(-112)
	48.8428	0.3936	1.86467	22.2	(-202)
	52.3429	0.492	1.74792	18.0	(020)
	58.0646	0.3936	1.58857	23.1	(202)
	61.3641	0.5904	1.51083	15.6	(-113)
	74.5893	0.4428	1.27235	22.6	(004)

DOI: *HTTPS://DOI.ORG/10.25130/TJPS.V31I3.1949*

FESEM Analysis

Figure 3 shows the results of FESEM of the prepared copper oxide nanoparticles. Most of the obtained NPs across all laser energies have individualized, ubiquitous forms as aggregates and agglomerations of less than 100 nm. These measurements show irregular geometric structures with average diameters (22.153, 25.79 and 20.664 nm) of NPs prepared at (100, 150, and 200 mJ), respectively. A decrease in average diameter was achieved due to increased energy.

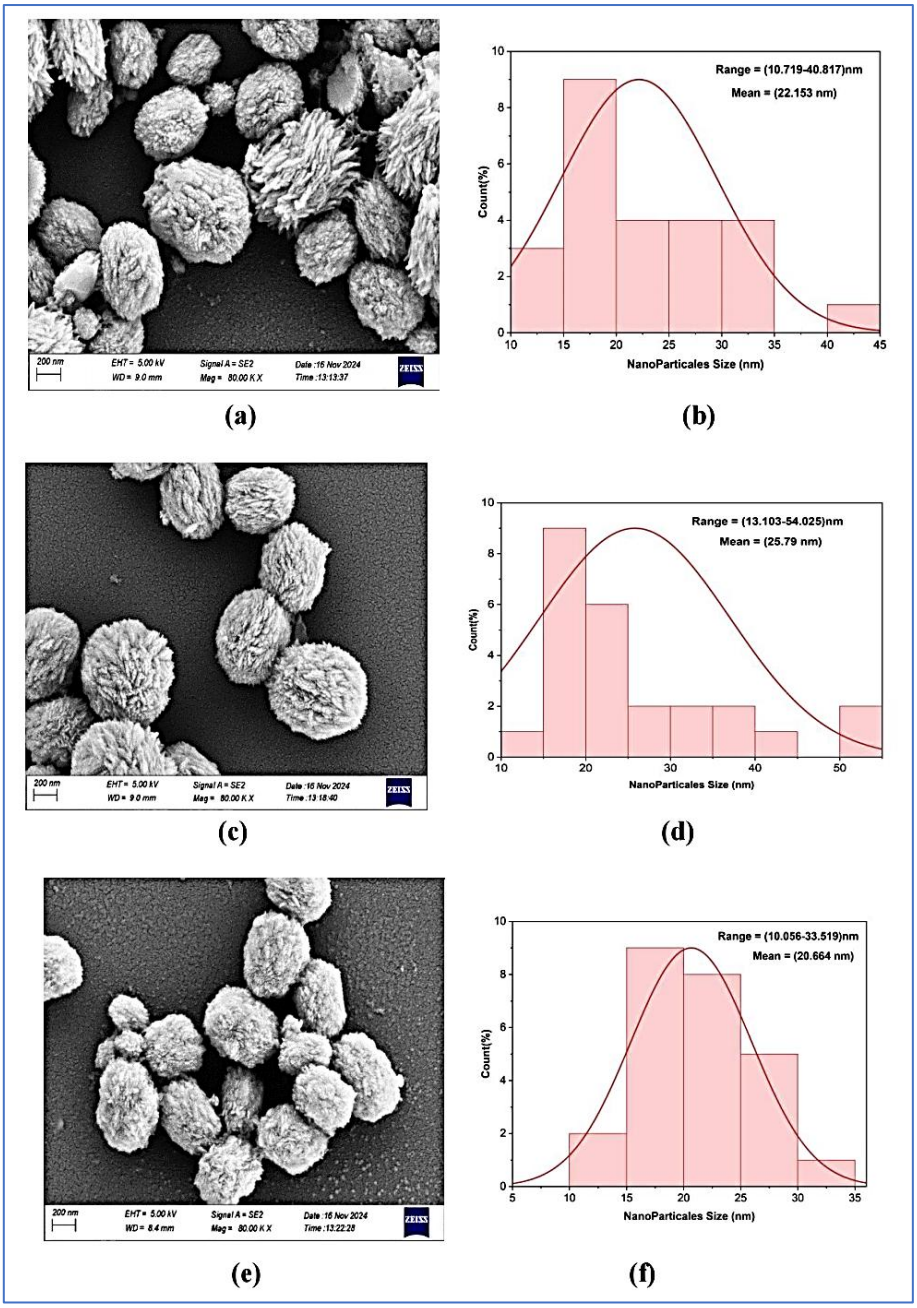

Fig. 3: FESEM results: (a) image of the prepared NPs at (100 mJ), (b) particle size statistical distribution of the prepared NPs at (100 mJ), (c) image of the prepared NPs at (150 mJ), (d) particle size statistical distribution of the prepared NPs at (150 mJ), (e) image of the prepared NPs at (200 mJ), (f) particle size statistical distribution of the prepared NPs at (200 mJ).

Optical Properties

Figure 4 shows the results of the absorption curves of the prepared NPs. It was observed that samples manufactured in deionized water exhibit a specific peak at 296 nm across all energies, consistent with previous studies. [11]. Absorption increased with the increase in laser energy.

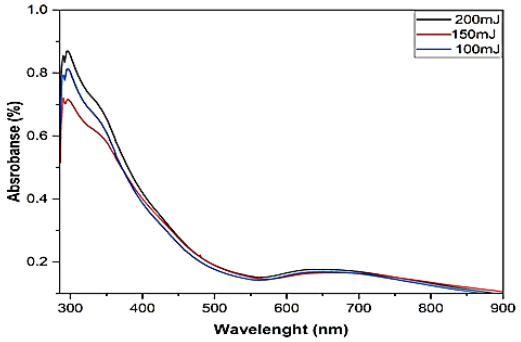

Fig. 4: Absorption spectra of the prepared CuO NPs.

Figure 5 shows the energy gaps of all the prepared NPs, obtained by plotting the Tauc equation. [12]:

$$(\alpha h\nu)^2 = B(h\nu - Eg)^{\frac{1}{2}} \quad \dots (3)$$

Where α is the absorption coefficient, hυ represents the photon energy, B is a constant of proportionality that depends on the type of material, and Eg is the energy gap. The energy gap is drawn using the software (Origin Pro 2025). The values of the energy gaps of copper oxide nanoparticles decreased with increased laser energy by (2.6 – 2.53 eV) [13].

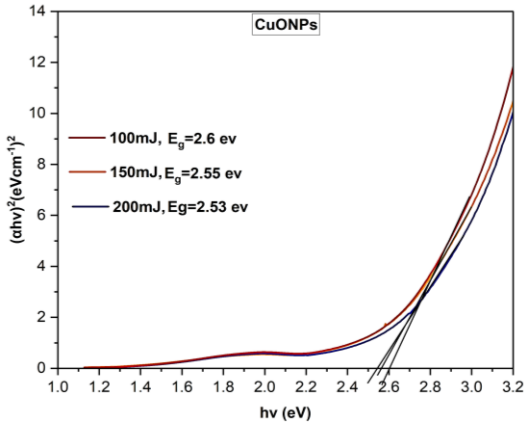

Fig. 5: Energy gap values of the prepared CuO NPs.

CONCLUSION

Copper oxide nanoparticles can be formed using the wavelength (532 nm). Changing the laser energy on the prepared CuO NPs samples increased the absorption values while maintaining a specific peak of absorption at the wavelength (296 nm). The energy gap values for the excised samples range from (2.6 - 2.53 eV) with increasing laser energy effect. This study can be further developed by varying the laser parameters and using a different laser to evaluate its effect on the properties of the applied materials.

Conflict of Interest: The authors declare no conflicts of interest related to this research.

Funding: This study received no specific funding from public, commercial, or non-profit funding agencies.

Author Contributions: All authors contributed equally to the preparation and completion of this work.

REFERENCES

1. Kittel C, McEuen P. Introduction to solid state physics: John Wiley & Sons; 2018.
2. Razzaq AA, Al-Nafiey A, Al-Marzoqy A. Decorated chitosan with silver-zinc nanoparticles by pulse laser ablation. Results in Optics. 2022;9:100282. https://doi.org/10.1016/j.rio.2022.100282
3. Dhiab S, Hassan NK. Study the Effect of Copper Oxide Nanorods Enhanced by Silver Nanoparticles on the Highly Sensitive Gas Sensor. Tikrit Journal of Pure Science. 2024;29(2):67-73. https://doi.org/10.25130/tjps.v29i2.1521
4. Subhan A, Mourad A-HI, Al-Douri Y. Influence of laser process parameters, liquid medium, and external field on the synthesis of colloidal metal nanoparticles using pulsed laser ablation in liquid: a review. Nanomaterials. 2022;12(13):2144. https://doi.org/10.3390/nano12132144
5. Razooqi MA, Majeed ZN. The Effect of Copper Doping on Some Structural and Electrical Properties of Titanium Dioxide Nanofilms. Tikrit Journal of Pure Science. 2023;28(6):51-7. https://doi.org/10.25130/tjps.v28i6.1377
6. Liu M, Liu H-Q, Chu S, Peng R-F, Chu S-J. [0001]-Oriented InN Nanoleaves and Nanowires: Synthesis, Growth Mechanism and Optical

Properties. Acta Metallurgica Sinica (English Letters). 2016;29:820-6.
https://doi.org/10.1007/s40195-016-0456-4

7. Mohammed SA, Khashan KS, Jabir MS, Abdulameer FA, Sulaiman GM, Al-Omar MS, et al. Copper Oxide Nanoparticle-Decorated Carbon Nanoparticle Composite Colloidal Preparation through Laser Ablation for Antimicrobial and Antiproliferative Actions against Breast Cancer Cell Line, MCF-7. BioMed Research International. 2022;2022(1):9863616.
https://doi.org/10.1155/2022/9863616

8. Ahmed BS, Mohammad SJ, Mohammed GH. The Effect of Laser Energy on the Structural, Optical and Electrical Properties of CdO Nanomaterials Generated Using (PLD) Technology and Fabrication of a Gas Sensor. Tikrit Journal of Pure Science. 2024;29(1):107-18.
http://dx.doi.org/10.25130/tjps.v29i1.1451

9. Saeed AA. Structural and Optical Properties of ZnO Nanoparticles for Antibacterial Application. Tikrit Journal of Pure Science. 2025;30(1):62-70.
https://doi.org/10.25130/tjps.v30i1.1779

10. Sultan AH, Saleh RF. Bioactivity of Gold Nanoparticles Synthesized from Lion's Mushroom on Multidrug-Resistant (MDR) ESKAPE Bacterial Isolates. Tikrit Journal of Pure Science. 2025;30(1):9-20.
https://doi.org/10.25130/tjps.v30i1.1692

11. Hathwara S, Devi BL, Ramananda D. Optical and Dielectric Properties of Poly (Vinyl Pyrrolidone-co-Vinyl Acetate)-Capped ZnS Nanoparticles. Journal of Electronic Materials. 2021;50(8):5007-12.
https://doi.org/10.1007/s11664-021-09026-z

12. Skiba M, Vorobyova V, Pasenko O. Surface modification of titanium dioxide with silver nanoparticles for application in photocatalysis. Applied Nanoscience. 2022;12(4):1175-82.
https://doi.org/10.1007/s13204-021-01739-1

13. Prasetya OD, Khumaeni A, editors. Synthesis of colloidal platinum nanoparticles using the pulse laser ablation method. AIP Conference Proceedings; 2018: AIP Publishing.
https://doi.org/10.1063/1.5054454